

## PULSAR TIMING. I. OBSERVATIONS FROM 1970 TO 1978

DAVID J. HELFAND

Department of Physics and Astronomy, University of Massachusetts; and  
 Columbia Astrophysics Laboratory, Columbia University

AND

J. H. TAYLOR, P. R. BACKUS, AND J. M. CORDES

Department of Physics and Astronomy, University of Massachusetts

Received 1979 May 21; accepted 1979 October 8

### ABSTRACT

The results of arrival time measurements of 37 pulsars are presented. Periods, period derivatives, positions, and proper motions are tabulated, and limits are placed on dispersion measure variations. A qualitative description of timing noise—which appears to be a general characteristic of pulsars—is made.

*Subject headings:* pulsars

### I. PULSAR TIMING

Much of what is known about neutron stars has been derived from precision timing measurements of pulsars. While it was the remarkable regularity of the pulsations that helped lead to the discovery of pulsars, it has been the small variations of the pulse rate that have contributed to an understanding of their physical nature. It was the secular decrease of the rotation rate of the Crab pulsar (PSR 0531+21) (Richards and Comella 1969) that first made clear the association of pulsars with neutron stars. The fact that most pulsars are spinning down on time scales of  $10^3$ – $10^{9.5}$  yr has led to inferred magnetic field strengths of  $10^{11}$ – $10^{13}$  gauss at the surfaces of neutron stars. Finally, the random variations in the spin rate, which are of two varieties, have provided information on the internal structure of neutron stars. Since 1969 March, the Vela pulsar (PSR 0833–45) has suddenly increased its rotation frequency 4 times by the amount  $\Delta\nu/\nu \approx 2 \times 10^{-6}$  (Radhakrishnan and Manchester 1969; Reichley and Downs 1969, 1971; Manchester, Goss, and Hamilton 1976; Downs 1978). Similar discontinuities or glitches have been observed twice in the Crab pulsar ( $\Delta\nu/\nu \approx 10^{-8}$  to  $10^{-9}$ ) (Papaliolios, Carleton, and Horowitz 1970; Boynton *et al.* 1972; Lohsen 1975; Helfand 1977) and in the longer period source, PSR 1641–45 (Manchester *et al.* 1978) with  $\Delta\nu/\nu \approx 2 \times 10^{-7}$ . The properties of these glitches, especially the relaxation of the rotation frequency to slightly less than its extrapolated preglitch value, have led to the view that neutron stars are multicomponent objects and that glitches are a result of the interchange of angular momentum between the crust and a more rapidly rotating, possibly superfluid neutron interior. The second kind of irregularity is the “timing noise” phenomenon manifested by random fluctuations in the rotational phase. Timing noise in the Crab pulsar was first investigated by Boynton *et al.* (1972) who concluded that the large phase residuals remaining after removal of a low-order polynomial (which ap-

proximates the deterministic spin-down) was the result of a random walk in the rotation frequency. A more complete analysis by Groth (1975*a, b, c*) on 5 years of timing data on the Crab pulsar confirmed this result. Qualitatively similar timing noise was recognized in a few longer period pulsars (Manchester and Taylor 1974) and, with the steadily accumulating data base, has recently been established as a general characteristic of pulsar timing behavior (Helfand 1977; Gullahorn 1979). This phenomenon may prove to be a sensitive probe of neutron-star structure and/or of the interaction of the star with its environment (Lamb, Pines, and Shaham 1978; Greenstein 1979; Gullahorn and Rankin 1980). Much of the work described herein has been done in light of this potential usefulness.

This paper is the first in a series in which we shall present the results of an 8-year program of pulsar timing. Multifrequency data for 37 sources have been analyzed to determine pulse periods and period derivatives, pulsar positions and proper motions, and the strength and character of timing noise. In the present paper, we report the observational results, including the fitted timing and astrometric parameters, and discuss the data analysis. We have also established limits on possible dispersion measure changes. In Paper II (Cordes 1980) we present a new mathematical procedure for the analysis of pulsar timing noise, while Paper III (Cordes and Helfand 1980) gives the results of its application to the data and an interpretation in the context of pulsar and neutron star models.

### II. OBSERVATIONS

Pulse arrival times reported here were collected as part of three pulsar observing programs. The first extended from early 1970 until mid-1973 and was conducted primarily by R. N. Manchester at the National Radio Astronomy Observatory (NRAO).<sup>1</sup> Observations were made at frequencies between 365

<sup>1</sup> Operated by Associated Universities, Inc., under contract with the National Science Foundation.

TABLE 1  
SUMMARY OF PULSE ARRIVAL TIME MEASUREMENTS

PSR (1)	Length of Data Span (days) (2)	Number of Measure- ments (3)	Typical Measure- ment Un- certainty (ms) (4)	RMS Residual (ms) (5)
0031+07...	2487	58	1.9	2.8
0301+19...	1834	67	0.6	0.9
0329+54...	2858	252	0.5	2.1
0355+54...	1862	52	0.5	0.7
0450-18...	1646	64	1.7	2.4
0525+21...	2224	64	2.2	2.2
0540+23...	343	30	0.4	0.3
0611+32...	1584	93	0.9	107.4
0809+74...	2777	66	0.9	1.3
0818-13...	2174	53	0.6	0.6
0823+26...	1833	130	0.6	11.9
0834+06...	2556	67	0.2	0.2
0950+08...	2560	97	0.2	0.2
1133+16...	2944	227	0.3	0.5
1237+25...	2599	121	0.3	0.5
1508+55...	2864	190	0.5	5.3
1604-00...	2176	69	0.3	0.4
1642-03...	2560	128	0.2	2.5
1706-16...	2560	89	0.3	7.9
1818-04...	2560	95	0.3	5.3
1911-04...	2557	51	0.2	0.6
1919+21...	2791	128	0.5	0.5
1929+10...	2576	31	0.2	0.3
1933+16...	2762	47	0.2	0.6
1944+17...	498	22	0.4	0.7
1946+35...	703	21	0.4	0.5
2002+31...	489	39	0.6	0.9
2016+28...	2789	127	0.4	0.5
2020+28...	2045	62	0.2	0.5
2021+51...	2585	50	0.3	4.7
2045-16...	2586	75	0.5	0.5
2111+46...	2457	63	2.1	2.1
2154+40...	1648	46	1.4	1.8
2217+47...	2864	208	0.6	0.9
2255+58...	489	47	6.0	6.0
2303+30...	2173	33	1.8	2.5
2319+60...	1577	37	1.1	2.0

MHz and 500 MHz using the 92 m transit telescope and an observing system described by Manchester (1971). Several total-intensity, integrated pulse profiles were recorded for each source in each of 15 observing sessions spaced at roughly two- to three-month intervals. A second data set derives from another NRAO program initiated by the present authors in 1975 October. It includes the measurement of pulse arrival times for 25 pulsars observed every few months at 410 MHz and/or 610 MHz, using a receiving system similar to that employed in the first program.

While these relatively coarsely sampled data have been extremely useful in extending our analysis over a longer baseline and a larger source sample, it is the data from the long-term pulsar program at the Five College Radio Astronomy Observatory (FCRAO) which forms the basis of this work. The Observatory's meter-wave telescope is currently configured as a dual-frequency, dual-polarization, four-element phased array operating at frequencies of 156 MHz and 390 MHz. The equipment configuration has undergone significant evolution since timing observations began

in July of 1973; here we describe only the broad outlines of the data acquisition and reduction scheme. Further details are discussed by Helfand (1977).

Throughout most of the period covered in this report, data were recorded at the FCRAO at one or both frequencies, several times a week, for each of seven pulsars. During 1976-1978, another dozen objects were added to the schedule. An observation usually consisted of 5 to 30 five-minute integrations. Either total intensity or circular polarization was employed, to eliminate the effects of the strong linear polarization of some of the sources. The five-minute averages were edited and combined to yield a single integrated pulse profile at each frequency, from which arrival times were determined as described in § III.

Table 1 presents a catalog of the arrival time data for 37 pulsars which resulted from these three programs. The pulsar names are listed in column (1). Column (2) lists the number of days spanned by the observations, and column (3) indicates the number of arrival times used in the analysis discussed below. The NRAO data often consist of several measurements concentrated in a period of less than a week, followed by a hiatus of 2 to 3 months. The FCRAO data are much more uniformly sampled, except for a few gaps (up to several weeks) caused by equipment problems or installation of new apparatus. In general, the arrival times have been recorded several times per week throughout the 4½ years covered by the program. The FCRAO arrival times were averaged in 15-day blocks; these averages were used in further analysis.

Column (4) of Table 1 lists our estimates of the typical measurement uncertainties of the daily observations. They are of the order of 0.5 ms, with variation about this value dependent on such factors as the pulse width, the resolution employed (which is often limited by dispersion smearing within the observing bandwidth), and the signal-to-noise ratio of the data. They were calculated by removing a local polynomial trend from the residuals and finding the rms deviation from the trend, as described in Paper II. Because of the different observing systems used and the continuous evolution of the FCRAO system, these errors are not uniformly applicable to all data on a source; rather, they are meant to characterize the data set as a whole and are useful in calculating the estimates of timing noise strengths derived in Paper III. The last column in Table 1 gives the rms arrival time residual, described in § IV.

### III. ARRIVAL TIME DETERMINATIONS

In determining pulse arrival times from the integrated profiles and fitting these times to an equation representing the secular slowdown of the spinning neutron star, we have followed a procedure similar to that described by Manchester and Peters (1972). We assume that the integrated pulse profile represents a fiducial marker attached to the surface of the neutron star and that it can be used to measure the time at which a fixed point of the star passes through the line of sight. It has been shown (Helfand, Manchester, and Taylor 1975) that pulsar integrated profiles usually

have stable profile shapes, if a sufficient number of pulses (typically a few hundred to a few thousand) are averaged. The problem, then, is reduced to one of measuring the time of occurrence of some specified feature (e.g., the peak) on the daily integrated profiles. This is accomplished by cross-correlating a "standard profile" (formed by averaging many individual integrated profiles for the same source) with the daily profiles.

Examples of typical, daily average profiles and standard profiles are shown in Figure 1 for two pulsars. The lag at which the cross-correlation function maximizes is taken as the arrival time of the pulse at the midpoint of the observation period. In practice, a parabola is fit to the peak portion of the correlation function to obtain the lag of maximum correlation, with an accuracy of about 0.1–1.0 sample intervals, depending on the signal-to-noise ratio and the pulse shape. PSR 1237+25 exemplifies the fact that some pulsars have average profiles that stabilize much more slowly than most because of mode changes in which the average profile switches between two shapes. The switching time is less than one pulse period and the profile stays in one of the states for several hundred or more pulses. Figure 1 shows that, although different from the standard profile, the profile contaminated by mode changes still has components that peak at the same locations. Thus, errors in the arrival times caused by mode changes are second order for PSR 1237+25. Gullahorn (1978) has suggested, however, that several pulsars may have large timing errors due to mode changing.

The measured pulse arrival times are corrected for instrumental delays, for propagation to the solar-

system barycenter (using the MIT Lincoln Laboratory solar system ephemeris, version PEP 311), and to infinite frequency using the known dispersion constant (usually the value given by Taylor and Manchester 1975) for the source. The dual-frequency nature of the observations was designed in part to eliminate effects of the arrival times which would result from variations in a pulsar's dispersion measure. Results from this ancillary dispersion monitoring effort are presented in § VII.

#### IV. DETERMINATIONS OF PULSAR PARAMETERS

The set of barycentric pulse arrival times amount to a determination of the phase of the pulsar's rotation as a function of time,  $\phi(t)$ . This function may be modeled as

$$\phi(t) = \phi_0 + \nu t + \frac{1}{2}\dot{\nu}t^2 + \frac{1}{6}\ddot{\nu}t^3 + \dots + \phi_A(t, \alpha, \delta, \mu_\alpha, \mu_\delta) + \phi_R(t), \quad (1)$$

where the terms  $\nu$ ,  $\dot{\nu}$ ,  $\ddot{\nu}$ , etc., are the pulsar rotation frequency and its derivatives, the quantity  $\phi_A$  includes astrometric effects of the (possibly time-dependent) position of the source (which is derivable from the data because of the dependence of the barycentric corrections on the source coordinates), and  $\phi_R$  represents glitches and timing noise. The  $\phi_R$  term is not included explicitly in the fitting procedure; determination of its form is the subject of Paper II. In practice, one uses previously determined values of the various parameters, computes predicted arrival phases, subtracts these from the observed values, and then

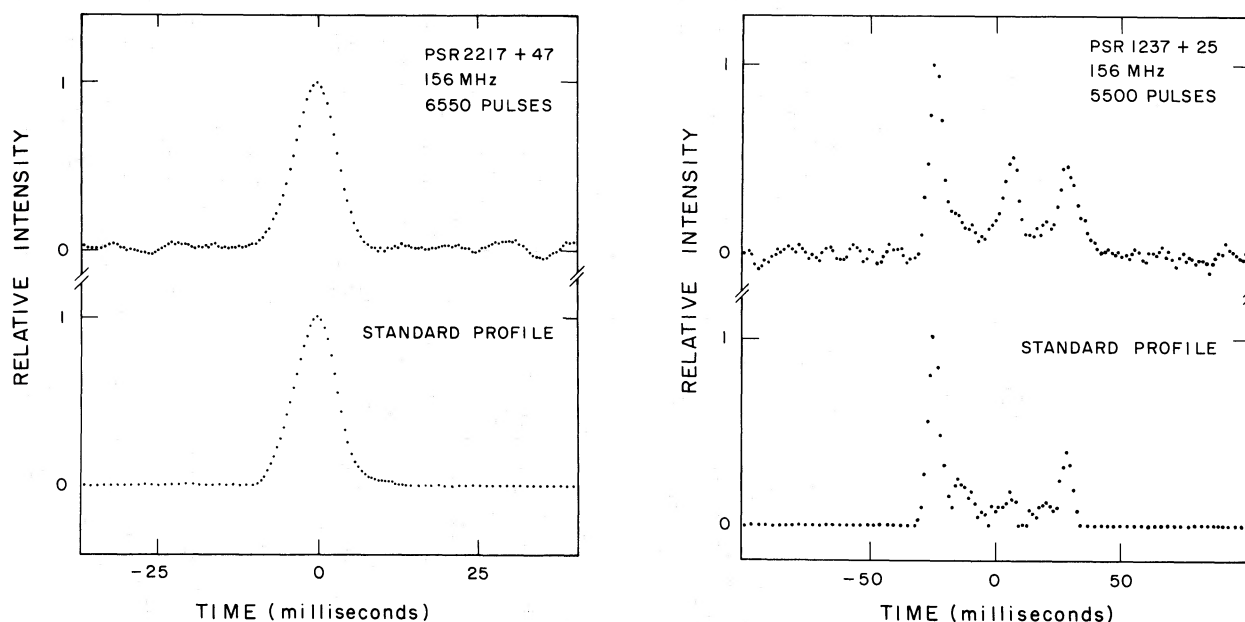


FIG. 1.—(a) Typical, daily-average intensity profile and standard profile for PSR 2217+47. Arrival time measurements are obtained by cross-correlating the standard profile with the daily average. (b) Same as Fig. 1a for PSR 1237+25. The shape difference between the two profiles is due to mode changes which alter the relative component amplitudes, possibly causing small errors in the arrival time determinations.

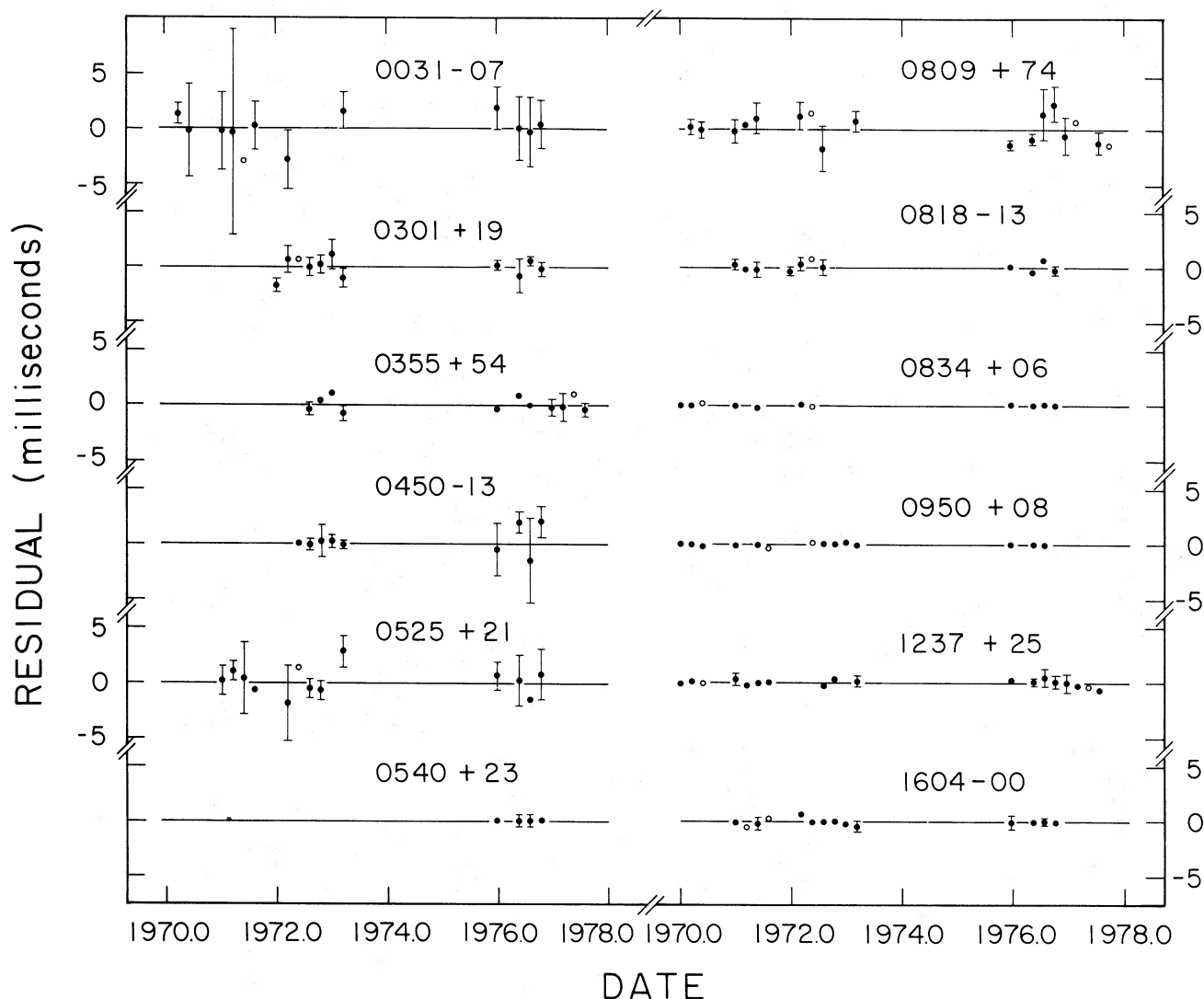


FIG. 2.—Phase residuals of 12 pulsars after fitting arrival times for the parameters in Table 2. Each plotted point is the mean of several measurements and an error bar (corresponding to  $\pm 1$  standard deviation) is shown, if it is larger than the plotted point. An open circle implies that only one measurement occurred in that time bin. A positive residual implies a late arrival time.

determines improved parameter estimates via a linearized least-squares procedure.

Parameter estimates for the entire data set are collected in Table 2. Pulsar periods, period derivatives, positions, and proper motions are listed in columns (2) through (7), respectively. Column (8) contains the epoch of the first observation for each source; the periods and positions are defined at this epoch. All quoted uncertainties are twice the formal standard error resulting from the least-squares fit. They do not explicitly take into account uncertainties introduced by the intrinsic noise process.

The last column in Table 1 presents the rms arrival time residuals after the slowdown polynomial and astrometric terms have been removed. A simple comparison of these values with the measurement uncertainties (column [4] in Table 1) indicates that for most

sources, significant phase residuals remain after accounting for the well-understood effects of spin-down, position offsets, and proper motion. These excess residuals, intrinsic to the pulsar rotation rate, are also apparent in Figures 2 through 4, where we have plotted the postfit timing residuals as a function of time. Quantitatively, these plots show a wide range of variations—some sources have phase residuals dominated by measurement uncertainty at a level of a few hundred microseconds, while others show dramatic phase excursions with amplitudes of up to  $\sim 0.2$  s. Qualitatively, however, all pulsars that show excess residuals follow a similar pattern, dominated by the quasi-sinusoidal structure first noted in the Crab pulsar by Boynton *et al.* (1972). This is characteristic of the pulsar timing noise phenomenon, and we devote Papers II and III to its analysis.

TABLE 2  
PARAMETERS FOR TIMING DATA

PSR	Period (s)	Period Derivative ( $10^{-15}$ s s $^{-1}$ )	Right Ascension (1950.0)	$\mu_{\alpha}$ cos $\delta$ ( $"$ yr $^{-1}$ )	Declination (1950.0)	$\mu_{\delta}$ ( $"$ yr $^{-1}$ )	Epoch (JD - 2440000.0)
0031-07	0.94295078490	$\pm 8$	00 <sup>h</sup> 31 <sup>m</sup> 36 <sup>s</sup> .4 $\pm 0.1$	0.1 $\pm 0.5$	-07°38'30"	-0.7 $\pm 1.4$	690.17
0301+19	1.38758355751	$\pm 6$	03 01 42.5 $\pm 0.1$	-0.8 $\pm 0.8$	19 21 10	2 $\pm 2$	1347.48
0329+54	0.71451866398	$\pm 1$	03 29 10.95 $\pm 0.04$	0.07 $\pm 0.08$	54 24 37.0	-0.1 $\pm 0.1$	621.50
0355+54	0.15638005591	$\pm 2$	03 55 00.39 $\pm 0.05$	0.13 $\pm 0.1$	54 04 42.8	-0.2 $\pm 0.2$	1593.85
0450-18	0.5489333679	$\pm 3$	04 50 21.1 $\pm 0.2$	1.4 $\pm 0.7$	-18 04 19.2	-0.3 $\pm 0.4$	1536.04
0525+21	3.7454934477	$\pm 2$	05 25 52.0 $\pm 0.1$	-0.4 $\pm 0.6$	21 57 04	7 $\pm 8$	957.65
0540+23	0.24596670036	$\pm 7$	05 40 06.9 $\pm 0.2$	---	23 28 04	---	2838.51
0611+22*	0.3349184451	$\pm 7$	06 11 15.59	---	22 29 14.0	---	1595.93
0809+74	1.29224132389	$\pm 4$	08 09 02.6 $\pm 0.1$	0.26 $\pm 0.13$	74 38 12.3	0.1 $\pm 0.1$	689.47
0818-13	1.23812810723	$\pm 2$	08 18 06.02 $\pm 0.02$	-0.01 $\pm 0.07$	-13 41 22.7	0.03 $\pm 0.08$	1006.64
0823+26	0.5306598025	$\pm 1$	08 23 50.3 $\pm 0.2$	---	26 47 10	---	1653.86
0834+06	1.273763535737	$\pm 8$	08 34 26.16 $\pm 0.01$	0.01 $\pm 0.03$	06 20 43.1	0.03 $\pm 0.08$	625.69
0950+08	0.2530650507263	$\pm 8$	09 50 30.58 $\pm 0.02$	-0.18 $\pm 0.06$	08 09 46.5	-0.41 $\pm 0.12$	621.77
1133+16	1.187911199667	$\pm 6$	11 33 27.44 $\pm 0.01$	-0.03 $\pm 0.04$	16 07 34.5	0.5 $\pm 0.1$	621.82
1237+25	1.382448613353	$\pm 9$	12 37 12.01 $\pm 0.01$	-0.08 $\pm 0.03$	25 10 17.0	0.00 $\pm 0.04$	625.87
1508+55	0.73967789893	$\pm 3$	15 08 03.79 $\pm 0.03$	0.01 $\pm 0.04$	55 42 54.8	0.11 $\pm 0.04$	625.96
1604-00	0.421816075804	$\pm 4$	16 04 37.80 $\pm 0.01$	-0.07 $\pm 0.04$	-00 24 40.9	-0.15 $\pm 0.12$	1005.95
1642-03	0.38768879136	$\pm 1$	16 42 24.68 $\pm 0.05$	-0.18 $\pm 0.16$	-03 12 31.7	0.2 $\pm 0.4$	622.04
1706-16	0.6530504733	$\pm 1$	17 06 33.3 $\pm 0.2$	-0.6 $\pm 0.8$	-16 36 43	-8 $\pm 5$	622.07
1818-04	0.59807263933	$\pm 6$	18 18 13.7 $\pm 0.1$	-0.2 $\pm 0.4$	-04 29 02	-1 $\pm 1$	622.10
1911-04	0.82593368969	$\pm 2$	19 11 15.19 $\pm 0.02$	-0.05 $\pm 0.06$	-04 46 00.4	0.23 $\pm 0.14$	624.13
1919+21	1.337301192264	$\pm 9$	19 19 36.16 $\pm 0.01$	0.02 $\pm 0.03$	21 47 16.1	0.04 $\pm 0.05$	689.95
1929+10	0.226517045140	$\pm 3$	19 29 51.88 $\pm 0.01$	0.10 $\pm 0.03$	10 53 03.7	-0.01 $\pm 0.04$	625.15
1933+16	0.35873543129	$\pm 1$	19 33 31.85 $\pm 0.03$	0.03 $\pm 0.08$	16 09 58.3	0.04 $\pm 0.09$	689.97
1944+17	0.44061846406	$\pm 5$	19 44 38.82 $\pm 0.02$	---	17 58 16.0	---	2693.50
1946+35	0.71730705200	$\pm 4$	19 46 33.95 $\pm 0.02$	---	35 32 38.1	---	2691.51
2002+31	2.1112194485	$\pm 2$	20 02 53.74 $\pm 0.02$	---	31 28 34.8	---	2691.52
2016+28	0.557953407278	$\pm 5$	20 16 00.14 $\pm 0.02$	-0.08 $\pm 0.05$	28 30 30.1	0.02 $\pm 0.05$	689.00
2020+28	0.343400791510	$\pm 4$	20 20 33.31 $\pm 0.01$	-0.05 $\pm 0.06$	28 44 43.2	-0.02 $\pm 0.07$	1348.19
2021+51	0.52919532782	$\pm 6$	20 21 25.3 $\pm 0.1$	---	51 45 07	---	625.17
2045-16	1.96156687983	$\pm 2$	20 45 46.9 $\pm 0.1$	0.3 $\pm 0.3$	-16 27 48	-0.9 $\pm 1.0$	695.01
2111+46	1.01468444504	$\pm 5$	21 11 37.77 $\pm 0.05$	---	46 31 42.3	---	1006.18
2154+40	1.5252633498	$\pm 8$	21 54 57.0 $\pm 0.2$	0.5 $\pm 0.5$	40 03 29	-0.6 $\pm 1.0$	1532.76
2217+47	0.538467394546	$\pm 5$	22 17 45.88 $\pm 0.02$	0.01 $\pm 0.05$	47 39 48.4	-0.05 $\pm 0.04$	624.26
2255+58	0.3682436648	$\pm 3$	22 55 45.7 $\pm 0.4$	---	58 54 22	---	2692.63
2303+30	1.5758844100	$\pm 4$	23 03 33.6 $\pm 0.4$	1.5 $\pm 1.5$	30 43 52	-1.2 $\pm 1.0$	1006.24
2319+60	2.256483705	$\pm 1$	23 19 41.4 $\pm 0.2$	0.2 $\pm 1.0$	60 08 03	-0.2 $\pm 1.0$	1535.82

\*Notes: 1. Uncertainties listed for periods and period derivatives refer to the last digit quoted.  
 2. For PSR 0611+22, the NRAO and FCRAO arrival times were augmented by 40 measurements from Arecibo Observatory, taken between 1973.1 and 1974.4. Because of the large intrinsic timing noise, no position solution was attempted for this source; the assumed position is consistent with the work of Gullahorn and Rankin (1978).  
 3. The proper motion of PSR 1508+55 was determined from data after 1972.6.

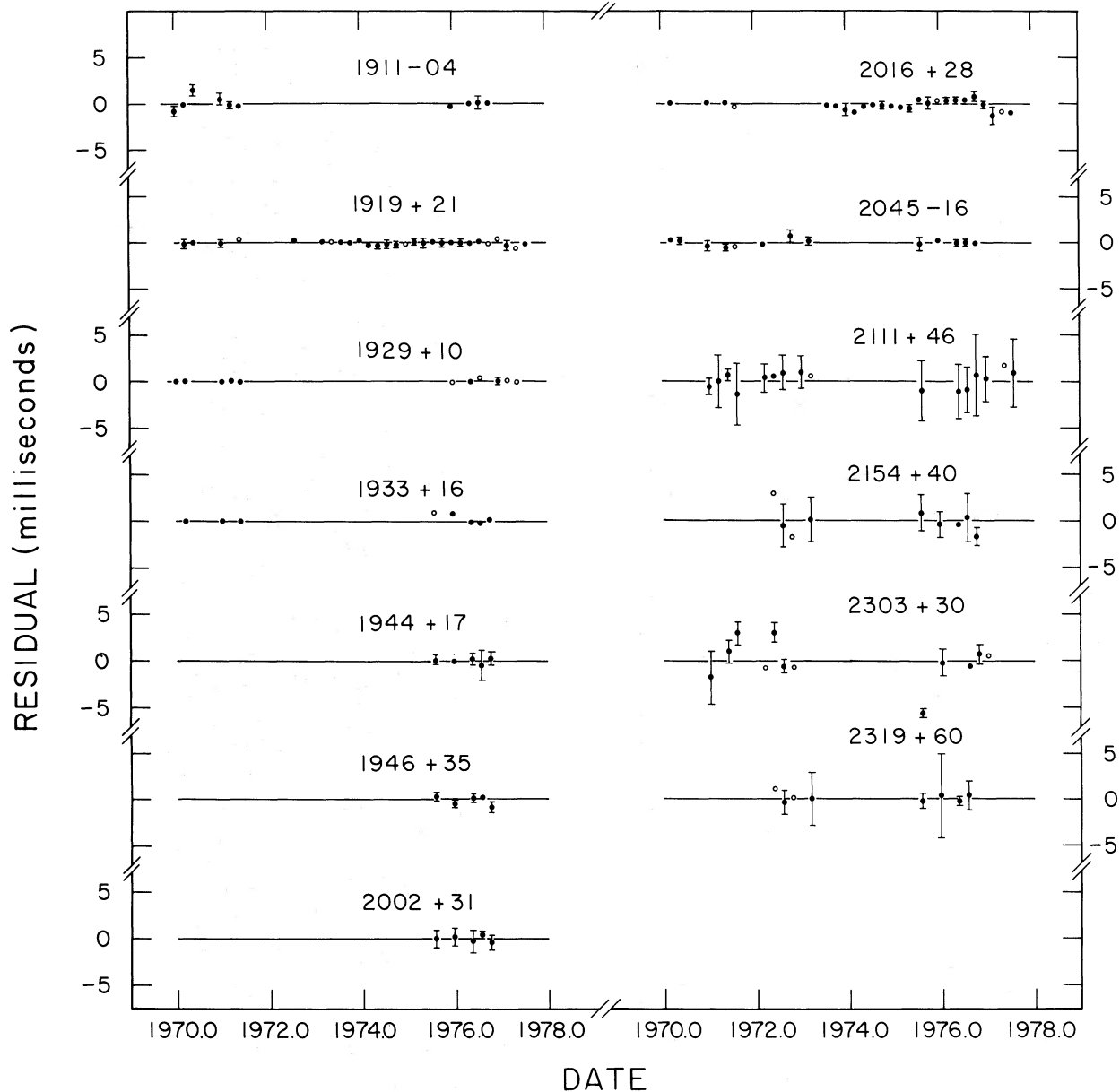


FIG. 3.—Same as Figure 2 for another 13 relatively inactive pulsars

#### V. PROPER-MOTION MEASUREMENTS

The measurement of proper motions is important to several areas of investigation concerning pulsars, including their ages, circumstances of origin, and birthrate. The first such measurement implies a transverse velocity of approximately  $100 \text{ km s}^{-1}$  for the optical pulsar in the Crab Nebula (Trimble 1971). Manchester, Taylor, and Van (1974) published the first radio-astronomical proper-motion measurement, based on pulse arrival time observations for PSR 1133+16. In this case, the measured angular motion corresponds to a velocity of about  $300 \text{ km s}^{-1}$ . More recently, interferometric techniques (Anderson, Lyne,

and Peckham 1975; Backer and Sramek 1976) have yielded proper motions for six additional pulsars, with inferred transverse velocities in the range from  $45$  to  $500 \text{ km s}^{-1}$ . Further measurements using pulse arrival time data have been presented by Helfand, Taylor, and Manchester (1977) and Gullahorn and Rankin (1978). Here we report the latest results from our data set, which includes measurements for three sources and useful upper limits for a dozen others.

One year of well-sampled pulsar timing data is usually sufficient to determine a source's position to within less than  $\sim 0''.2$ , as long as timing noise is negligible. Using the fitting procedure outlined in Manchester, Taylor, and Van (1974), we have obtained

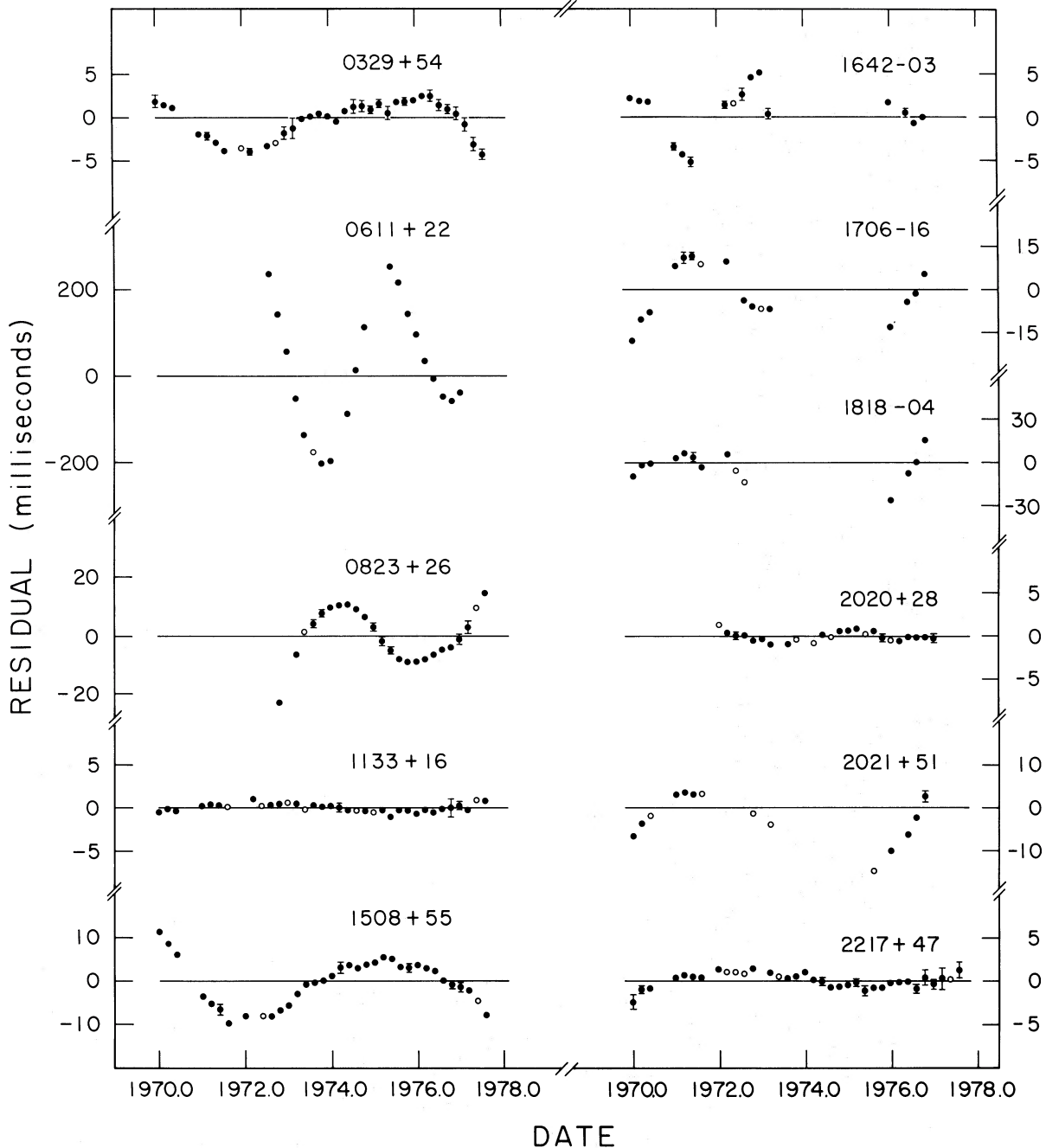


FIG. 4.—Phase residuals for 11 pulsars which show considerable timing noise activity

the proper motions listed in columns (5) and (7) of Table 2. The results for PSR 1133+16 and PSR 1508+55 agree with our previously published values based on shorter data spans and, in the first case, with interferometric and timing results from other authors. The measurements for PSR 1237+25 and PSR 1929+10 are our first determinations of proper motion for these sources. For PSR 1237+25 the results agree satisfactorily with other interferometric (Anderson, Lyne, and Peckham 1975) and timing (Gullahorn and Rankin 1978) results, but for PSR 1929+10 our re-

sults are not in accord with Gullahorn and Rankin. Most of the proper motions in Table 2 are, effectively, upper limits, since the uncertainties are larger than the nominal values. Here again, the results are generally consistent with other published values, although our upper limit for PSR 1919+21 is a factor of 3 below the detection claimed by Gullahorn and Rankin (1978). With a few more years of observations and the inclusion of earlier data from other programs (e.g., Gullahorn and Rankin 1978), it may be possible to solve for several more proper motions from among

the sources listed in Table 2. However, in most of the remaining cases the pulsar distance is probably too large, or the timing noise too dominant, for proper motions to be determined in this way.

Although based on a limited set of data, the proper-motion result for PSR 0450-18 is intriguing because of the pulsar's suggested association with a nearby extended X-ray source, tentatively identified by Narayan *et al.* (1976) as an old supernova remnant (SNR). The motion is directed away from the centroid of X-ray emission, with a position angle within  $20^\circ$  of the line joining the pulsar and the SNR center. The observed angular separation of  $10''.5$  and the angular proper-motion measurement of  $\sim 1''.4 \text{ yr}^{-1}$  allow us to determine the time since the pulsar left the remnant centroid, independently of the distance. If the pulsar and the SNR are related, the age of the SNR is  $3 \times 10^4$  years, or about twice the age of the similar X-ray remnants Vela X and the Cygnus Loop. For distances to the SNR in the range 100-300 pc (Narayan *et al.* 1976) the implied transverse velocity of the pulsar is a large (but not unphysical)  $650\text{--}2000 \text{ km s}^{-1}$ . The spin-down age  $\tau = P/2\dot{P}$  for PSR 0450-18 is  $\sim 2 \times 10^6 \text{ yr}$ . If the proper motion determined here is confirmed, and the association of the pulsar with the SNR can be substantiated, the wide discrepancy in the actual characteristic ages will imply that the pulsar must have been born rotating slowly. Such a conclusion has important implications in such areas as supernova collapse theory, pulsar acceleration mechanisms, and the birthrate and evolution of the galactic pulsar population.

## VI. GLITCHES AND FREQUENCY SECOND DERIVATIVES

### a) Glitches in Long-Period Pulsars

As noted in § I, there have been a number of reports of discontinuous changes in pulsar rotation frequencies commonly referred to as glitches. Five of these have occurred in the two youngest pulsars (the Crab and Vela sources) and exhibit the characteristic signature of an abrupt increase in both frequency and frequency derivative, followed by an exponential decay of the derivative to its original value. The result long after the glitch is a small, permanent frequency offset from the value extrapolated from the preglitch parameters. Attempts have been made to describe other features of the Crab pulsar timing history in terms of frequency discontinuities (Lohsen 1972; Nelson *et al.* 1970), but Groth (1975c) has argued that these "events," which did not exhibit all of the characteristic features described above, are more easily explained as manifestations of the noise process. In addition, there have been several reports of glitches occurring in old pulsars (Manchester and Taylor 1974; Gullahorn *et al.* 1976; Gullahorn and Rankin 1978). It is suggested below that these events also may be wanderings of the phase due to a stochastic noise process.

Figure 5 shows the timing residuals for PSR 0823+26 resulting from a fit to the FCRAO data for  $\phi_0$ ,  $\nu$ , and  $\dot{\nu}$ , up to the date indicated. The formal errors of the fitted parameters indicate that it should

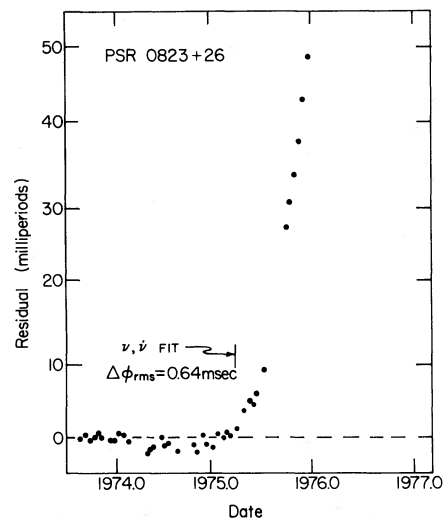


FIG. 5.—Phase residuals for PSR 0823+26 after a fit for  $\nu$  and  $\dot{\nu}$  over the time interval indicated.

be possible to predict the future arrival phases with an error of less than 50 milliperiods over  $\sim 2000$  days. It is clear, however, that within only  $\sim 200$  days, the error has grown to about 50 milliperiods and is increasing rapidly. If the data after the indicated date are fitted with a second-order polynomial, new values for  $\nu$  and  $\dot{\nu}$  will be found which differ from the earlier determinations by many times their combined formal errors. It is this kind of analysis procedure which has led to some claims of glitch detections in old pulsars.

Several aspects of these events do not fit the classical glitch format, however. In this instance, the arrival phases are becoming more positive with time (i.e., pulses are arriving late), indicating a sudden slowdown of the star, not a spin-up. For the case of PSR 1508+55 (Manchester and Taylor 1974), the sign of the frequency derivative change was also opposite to that observed in the glitches of younger sources, and for PSR 1906+00 (Gullahorn *et al.* 1976), there did not appear to be as sharp a kink in the residual curve as that characteristic of the Crab and Vela discontinuities. Figure 6 presents the residuals calculated from the same timing data shown in Figure 5, but with the fit extending through the end of the data string. The date at which the glitch appeared in the previous fit is marked with an arrow. There is no indication of any noncontinuous behavior at this (or any other) time. The form of the residuals closely resembles that described by Boynton *et al.* (1972) for the Crab residuals: quasi-sinusoidal structure with a dominant wavelength comparable to the data span.

Clearly, these data could be divided at any place within 200 days of the arrow and fitted with two second-order polynomials with different coefficients, greatly reducing the phase residuals. There appears, however, to be no physical justification for this procedure. Boynton *et al.* (1972) have explicitly shown that the random superposition of many small steps can lead to apparent, large slope discontinuities such as that shown in Figure 5. The explanation of this

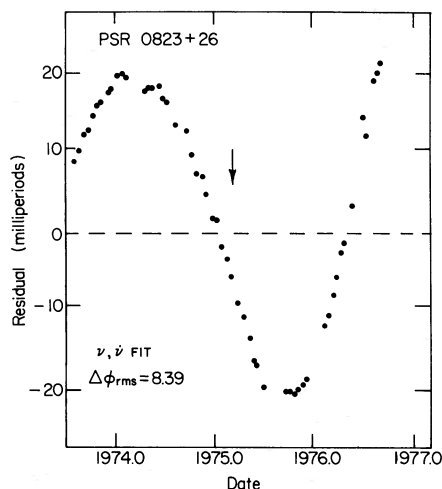


FIG. 6.—Phase residuals for PSR 0823+26 after a fit for  $\nu$  and  $\dot{\nu}$  to all the FCRAO data.

residual pattern in terms of such a random walk process is pursued in Paper III.

An alternative method for reducing the residuals of the fit to PSR 0823+26 would be to add another term, proportional to  $t^3$ , to the slowdown polynomial. The coefficient of this term represents the frequency second derivative,  $\ddot{\nu}$ , and can be used to determine the so-called braking index,  $n$ , defined by

$$n = \nu \ddot{\nu} / \dot{\nu}^2. \quad (2)$$

The results of a third-order fit appear in Figure 7; the residuals have been reduced by a factor of 5, and they are now dominated by a fourth-order polynomial. This implies that a low-order polynomial (of order 4 or smaller) is not a good model for the data. Moreover, the value of  $\ddot{\nu}$  obtained from the fit implies a braking index of nearly  $-10^4$ , which is not realistic for the torque processes that are thought to be relevant. One interpretation, of course, is that a glitch—whose phase signature is markedly different from glitches observed from the Crab and Vela pulsars—has occurred. However, the results are very similar to those expected from a random walk process, which produces residuals with both small- and large-order polynomial components (Groth 1975*b*; Paper III).

According to equation (2), pulsars with the largest values of  $\dot{\nu}$  will be those most likely to have measurable values of  $\ddot{\nu}$  over a given time span. The best candidate of our pulsars is therefore PSR 0611+22, but it also displays large residuals after a third-order fit, and like PSR 0823+23, the implied braking index ( $\sim 350$ ) is also embarrassingly large. Other pulsars with large values of  $\dot{\nu}$  include PSRs 0153+61, 1727-47, and 1930+22, but few timing data have been accumulated for them so far. It thus appears that no frequency second derivatives will be measurable for many years to come, except possibly for the Vela pulsar (PSR 0833-45). In Paper III, we find that timing noise is generally correlated with  $\dot{\nu}$ , further evidence for our pessimistic conclusion.

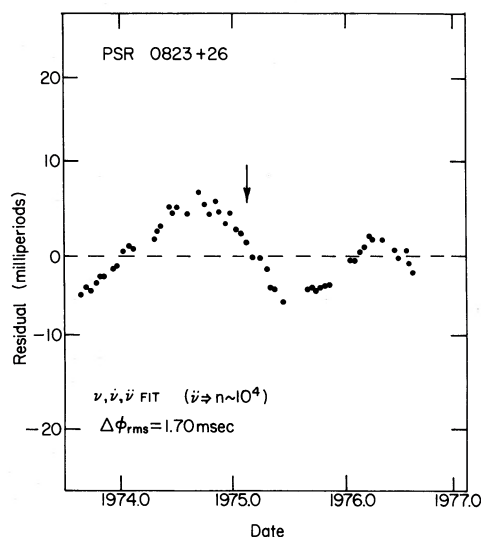


FIG. 7.—Phase residuals for PSR 0823+26 after a fit for  $\nu$ ,  $\dot{\nu}$ , and  $\ddot{\nu}$  to all the FCRAO data.

#### VII. LIMITS ON DISPERSION MEASURE VARIATIONS

Simultaneous dual-frequency observations of seven pulsars have been conducted since 1973 at the FCRAO. In principle, these observations allow detection of dispersion variations that cause time shifts larger than the random errors of the pulse arrival times. Marginally significant variations as large as  $\sim 1$  ms were sometimes observed between 156 and 390 MHz, but these appear as a systematic trend over the 8-year data span and apparently can be associated with the 390 MHz data only. We believe that the trend must have an instrumental origin, because it was not evident in a comparison of our 156 MHz measurements with data obtained at 430 MHz at the Arecibo Observatory. Consequently, our limit on dispersion variations is  $\Delta DM \lesssim 7 \times 10^{-3} \text{ pc cm}^{-3}$  for PSRs 0329+54, 0823+26, 1133+16, 1508+55, 1919+21, 2016+28, and 2217+47.

#### VIII. SUMMARY

We have presented the results of a series of pulsar timing programs spanning eight years. The data have yielded accurate periods, period derivatives, and positions for three-dozen sources. Proper motions for three pulsars have been determined, useful upper limits have been derived for most of the remaining objects, and limits have been placed on possible dispersion measure changes. The timing noise phenomenon, first seen in the Crab pulsar, has been established as a general characteristic of pulsar rotation rates. As such, it is likely to be a useful tool in the investigation of problems in neutron-star structure and pulsar evolution, and the analysis and interpretation of this feature of the data will be the subject of subsequent papers in this series.

We thank R. N. Manchester for his invaluable participation in the early phases of these observations,

G. Gullahorn and J. Rankin for supplying data in advance of publication, and the staff of the Five College Radio Astronomy Observatory for continued support during all phases of this work. The FCRAO is operated with support from the National Science

Foundation under grant AST 76-24610 and with the permission of the Metropolitan District Commission, Commonwealth of Massachusetts. This paper is contribution number 308 of the Five College Observatories.

## REFERENCES

- Anderson, B., Lyne, A. G., and Peckham, R. J. 1975, *Nature*, **258**, 215.
- Backer, D. C., and Sramek, R. A. 1976, *A.J.*, **81**, 430.
- Boynton, P. E., Groth, E. J., Hutchinson, D. P., Nanos, G. P., Jr., Partridge, R. B., and Wilkinson, D. T. 1972, *Ap. J.*, **175**, 217.
- Cordes, J. M. 1980, *Ap. J.*, submitted (Paper II).
- Cordes, J. M., and Helfand, D. J. 1980, *Ap. J.*, in press (Paper III).
- Downs, G. S. 1978, IAU Circ. No. 3274.
- Greenstein, G. 1979, *Ap. J.*, **231**, 880.
- Groth, E. J. 1975a, *Ap. J. Suppl.*, **29**, 431.
- . 1975b, *Ap. J. Suppl.*, **29**, 443.
- . 1975c, *Ap. J. Suppl.*, **29**, 453.
- Gullahorn, G. E. 1979, Ph.D. thesis, Cornell University.
- Gullahorn, G. E., Payne, R. R., Rankin, J. M., and Richards, D. W. 1976, *Ap. J. (Letters)*, **205**, L151.
- Gullahorn, G. E., and Rankin, J. M. 1978, *A.J.*, **83**, 1219.
- . 1980, in preparation.
- Helfand, D. J. 1977, Ph.D. thesis, University of Massachusetts.
- Helfand, D. J., Manchester, R. N., and Taylor, J. H. 1975, *Ap. J.*, **198**, 661.
- Helfand, D. J., Taylor, J. H., and Manchester, R. N. 1977, *Ap. J. (Letters)*, **213**, L1.
- Lamb, F., Pines, D., and Shaham, J. 1978, *Ap. J.*, **224**, 969.
- Lohsen, E. 1972, *Nature Phys. Sci.*, **236**, 70.
- . 1975, *Nature*, **258**, 689.
- Manchester, R. N. 1971, *Ap. J. Suppl.*, **23**, 283.
- Manchester, R. N., Goss, W. M., and Hamilton, P. A. 1976, *Nature*, **259**, 291.
- Manchester, R. N., Newton, L. M., Goss, W. M., and Hamilton, P. A. 1978, *M.N.R.A.S.*, **184**, 35P.
- Manchester, R. N., and Peters, W. L. 1972, *Ap. J.*, **173**, 221.
- Manchester, R. N., and Taylor, J. H. 1974, *Ap. J. (Letters)*, **191**, L63.
- Manchester, R. N., Taylor, J. H., and Van, Y. Y. 1974, *Ap. J. (Letters)*, **189**, L119.
- Naranan, S., Shulman, S., Friedman, H., and Fritz, G. 1976, *Ap. J.*, **208**, 718.
- Nelson, J., Hills, R., Cudaback, D., and Wampler, J. 1970, *Ap. J. (Letters)*, **161**, L235.
- Papaliolios, C., Carleton, N. P., and Horowitz, P. 1970, *Nature*, **228**, 445.
- Radhakrishnan, V. and Manchester, R. N. *Nature*, **222**, 228.
- Reichley, P. E., and Downs, G. S. 1969, *Nature*, **222**, 229.
- . 1971, *Nature*, **234**, 48.
- Richards, D. W., and Comella, J. M. 1969, *Nature*, **222**, 551.
- Taylor, J. H., and Manchester, R. N. 1975, *A.J.*, **80**, 794.
- Trimble, V. 1971, in *IAU Symposium 46, The Crab Nebula* (Dordrecht: Reidel), p. 3.

P. R. BACKUS and J. H. TAYLOR: Department of Physics and Astronomy, University of Massachusetts, Amherst, MA 01003

J. M. CORDES: Astronomy Department, Cornell University, Space Science Building, Ithaca, NY 14853

D. J. HELFAND: Astronomy Department, Columbia University, 538 W. 120th Street, New York, NY 10027